

# Auger Peaks in the Energy Spectra of Secondary Electrons from Various Materials

J. J. LANDER

Bell Telephone Laboratories, Murray Hill, New Jersey

(Received June 5, 1953)

The energy spectra of secondary electrons from carbon, beryllium, aluminum, nickel, copper, barium, platinum, and the oxides of beryllium, aluminum, nickel, copper, and barium have been measured with equipment of high stability and sensitivity. Characteristic peaks due to Auger electrons emitted as a result of absorption of a valence electron by an excited x-ray level were observed for all these materials.

The peaks exhibit structure which is of some theoretical interest. The structure can be related to the distribution in energy of electrons in the valence band, and it complements that observed in soft x-ray emission work. Since the emission of the Auger electron is not subject to the selection rules governing the emission of x-radiation, additional information can be obtained from the Auger electron energy distribution.

Excitation of Auger peaks by a beam of low velocity electrons provides an interesting technique for surface analysis.

"Plasma" peaks of the type reported by Ruthemann, and interpreted by Pines and Bohm, were also observed.

## 1. INTRODUCTION

CERTAIN discrete maxima in the energy spectra of secondary electrons excited by a primary beam of moderate voltage (roughly from one hundred to a few thousand volts) are the principal subject of this report. "Peaks" or "humps" of this type have been reported by others, but their nature has not been established.<sup>1</sup> The features, observed in distributions obtained by us from a number of materials, are attributed to Auger electrons emitted after excitation of x-ray levels by the primary beam or secondarily by x-radiation excited by the primary beam.

We will be concerned with the following process: an atom which has lost an electron from an inner level ( $K, L, \text{etc.}$ ) returns toward the normal state by absorption of an electron from an upper level (valence,  $K, \text{etc.}$ ) and the energy released in this transition appears in the form of an Auger electron ejected from a nearby upper level. These processes will be described, using the Skinner notation, as  $V \rightarrow K, V \rightarrow L, K \rightarrow L, \text{etc.}$  They complement those in which the energy balance is restored by emission of x-radiation. The selection rules governing the radiative process limits the information obtainable by the x-ray method. The Auger process is not subject to this limitation. For example, in the soft x-ray spectroscopy of carbon, the distribution of valence  $p$  electrons is largely reflected in the radiation distribution curve, whereas the Auger electron distribution curve should reflect the distribution of both  $p$  and  $s$  electrons.

Unfortunately the Auger electron distribution does not reflect the distribution of valence band electrons in a simple manner. Consider the three processes shown in Fig. 1. These all yield Auger electrons with energy  $W_K - 2W$ . Energy is here taken relative to that of an electron at rest in free space,  $-W_K$  is the energy of the

x-ray level involved in the process (here assumed to be a  $K$  level), and  $-W$  is the average of the initial energies of the two electrons.

To obtain an approximate distribution function for the Auger spectrum, assume that the probability of transitions yielding electrons in the energy range  $d(W_K - 2W)$  is proportional to the product of the densities in the regions  $dW'$  and  $dW''$  of the valence band, equidistant from  $W$ , and for which electron densities are given by a distribution function  $\rho(W)$ . The number of Auger electrons,  $dN$ , in the range  $d(W_K - 2W)$  can be obtained by integration with respect to  $\Delta W$ . The integration limits are  $W_a - W$  and zero if  $W$  is in the lower half of the band, or zero and  $W - \phi$  if  $W$  is in the

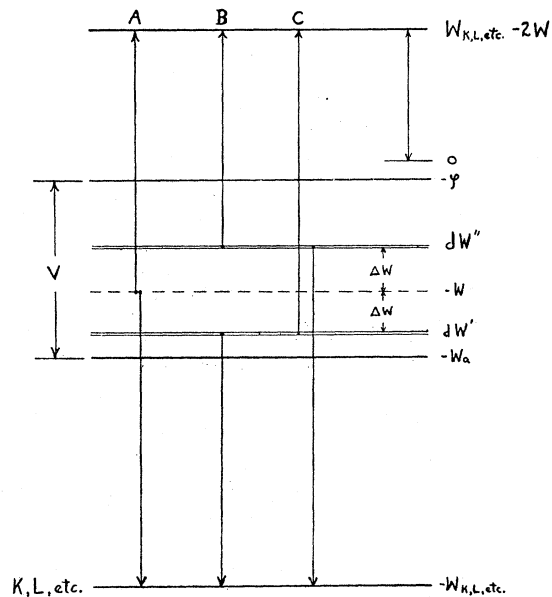


Fig. 1. Auger electron emission resulting from transitions of type  $V \rightarrow K, V \rightarrow L, \text{etc.}$  The three processes A, B, and C yield Auger electrons with equal energies.

<sup>1</sup> For a discussion of related work and appropriate references see the review article by K. G. McKay, *Advances in Electronics* (Academic Press, Inc., New York, 1948), pp. 72 and 83.

upper half. Thus,

$$dN(W_K - 2W)$$

$$\sim dW \int_{W_a - W}^0 \rho(W - \Delta W) \rho(W + \Delta W) d(\Delta W)$$

or

$$dW \int_0^{W - \varphi} \rho(W - \Delta W) \rho(W + \Delta W) d(\Delta W).$$

Integrals of the above type might be called Auger transforms. It is expected that more complicated expressions will be required for a generally satisfactory theory. For simply behaved materials it is clear that the energy range of the Auger distribution should be double that of the valence band. Commonly the maximum in  $\rho$  is in the upper part of the valence band. In this case the Auger distribution should also peak in the upper part of the spectrum and then fall to zero at a value (in the vacuum) equal to  $W_K - 2\varphi$ . The Auger spectrum will show much less detail than the soft x-ray spectrum.

Excitation of characteristic Auger electrons by x-radiation has been the subject of considerable investigation since the classic work of Auger.<sup>2</sup> A working analytical instrument based on this process has been described recently by Steinhardt and Serfass.<sup>3</sup> Excitation by an electron beam of moderate energy provides an experimental alternative with features of specific interest which will be discussed in the final section of this paper. Excitation of high energy processes by high energy electrons has been described by de Broglie and Thibaud.<sup>4</sup>

The spectra from numerous materials have been re-examined using equipment which was well stabilized and capable of good resolution and high sensitivity. The characteristic peaks observed have, in general, sufficient intensity to make the technique interesting as a means of surface analysis, and they show structure which is of some theoretical interest. Features observed in the low and high voltage regions of the energy distribution curves agree substantially with those reported by others and have not been described in detail. The literature is voluminous and the review of McKay is sufficiently comprehensive.

## 2. APPARATUS

Desirable features in the required equipment are high stability, high sensitivity, good resolution, and good vacuum conditions. The construction of the spherical electron analyzer used to obtain high sensitivity and of the electron gun used to obtain high stability (see Fig. 2) is somewhat novel. The principal items of apparatus are described briefly below.

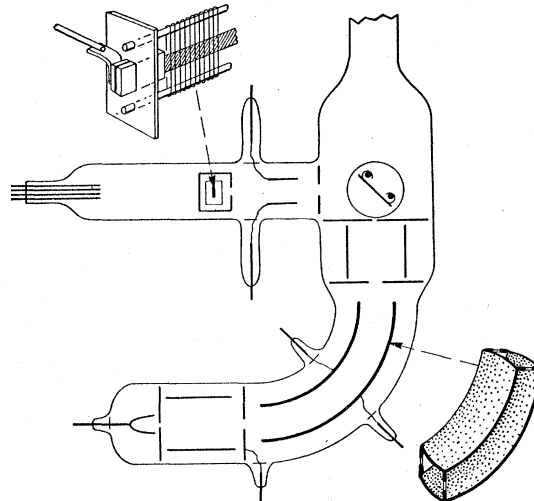


Fig. 2. Spherical electron velocity analyzer, electron gun, and target at 45° to gun and analyzer.

(a) The *beam voltage source* consisted of two 105- and nine 150-voltage regulator tubes in series across a filtered 2500-volt dc supply stabilized by drawing 10 milliamperes.

(b) The *electron gun* (see Fig. 2) was a tungsten ribbon filament 0.040 in. wide, 0.50 in. long, and 0.001 in. thick, welded to nickel leads and on which was floated a flattened 6AK5 grid by means of mica supports. A 0.050-in. hole in the surrounding rectangular plate defined the beam. Deflection, and to some extent focusing, was accomplished by adjusting voltages on the square box array of plates following this hole. Deflection voltages were supplied by a regulated source. The grid over the filament produced a triode with an average transconductance of about 1000 micromhos in the range of operation, which was normally with a cathode bias resistor of 20 000 ohms, a plate current of about 0.2 milliamperes and grid at about -4 volts. High beam current stabilization was thus obtained when the filament temperature was sufficiently high.

(c) The *velocity analyzer* (see Fig. 2) consisted of two 90° sections less one-half the gap distance at each end, cut from glass spheres coated with Aquadag, dimensions as shown in the drawing. Ten-mil object and twenty-mil image slits were located at distances from the analyzer plates equal to the average radius of curvature of the analyzer plates. The two-dimensional focusing principle of the spherical analyzer was used to obtain high sensitivity. The resolution of the instrument was better than one percent, as checked by measuring half-breadths of curves from elastically scattered primary electrons. In a preliminary stage of construction the collector and image slit were replaced by a fluorescent screen. It was found that the analyzer produced an excellent image of electrons drawn from a wide tungsten ribbon filament.

<sup>2</sup> P. Auger, *Compt. rend.* **180**, 65 (1925).

<sup>3</sup> R. G. Steinhardt and E. H. Serfass, *Anal. Chem.* **23**, 1585 (1951).

<sup>4</sup> M. de Broglie and H. Thibaud, *Compt. rend.* **180**, 179 (1925).

It is to be noted that the width in energy of the electrons passing through the image slit of this type of analyzer is proportional to their average energy. The curves shown in Figs. 3 and 4 have not been corrected for this effect.

(d) The *electrometer amplifier* has been described elsewhere.<sup>5</sup> Its limiting current sensitivity was about  $1 \times 10^{-15}$  ampere. Distribution curves were normally obtained by operating an Esterline Angus recording milliammeter with the output of the amplifier, the time axis being controlled by the recorder gears and the rate of sweep.

(e) The *sweep* voltage was obtained from regulated circuitry which provided for manual selection or automatic sweep at selected rates. A rate of about two volts per second was found convenient for most studies. Sweep voltages were read on a calibrated meter with an accuracy of about 0.2 percent, and were subsequently converted to electron energy using the analyzer constant obtained from measurements of high voltage elastically scattered primary beams of measured voltage.

(f) The *target* (see Fig. 2): One or more targets set at  $45^\circ$  to the primary beam and to the analyzer were supported on a tungsten wire frame. They could be moved into position magnetically along the horizontal axis of the target so that exposure under high vacuum to one of several sources of evaporating material in attached tubes was feasible. They were demagnetized before analysis. In various phases of the work, copper, platinum, and nickel targets were used, either for direct analysis or as substrates for other materials.

It was apparent from tests which were made that space charge distortion affected the distributions obtained in the range below about 15 volts. This distortion

is a function of the analyzer construction as well as that of the target and slit system. It is of no importance to the interpretation of results which will be discussed.

(g) The *vacuum system* consisted of Pyrex glassware, mechanical pump, a two-stage mercury pump, and two liquid air traps. Bake-out procedures which produced pressures of about  $1 \times 10^{-8}$  mm of Hg were used.

### 3. EXPERIMENTAL RESULTS AND INTERPRETATION

The materials investigated were carbon, beryllium, aluminum, nickel, barium, copper, platinum, and the oxides of beryllium, aluminum, nickel, barium, and copper. Quantitative data are given in the summary of measurements in Table I. The measurements and their interpretation are discussed for each material in the following subsections.

#### 3.1 Carbon

Carbon was applied to a nickel target in the form of a sprayed Aquadag coating. It was also unintentionally deposited and observed (with identical results) on several surfaces after primary beam bombardment for many minutes, while the pressure in the vacuum system was in the  $10^{-6}$  and  $10^{-7}$  mm of Hg range. A representative distribution curve is given in Fig. 3 with the carbon feature enlarged and compared with the carbon *K* x-ray emission curve (due largely to *p* electrons) given by Skinner.<sup>6</sup>

Note that a curve corrected to give number of electrons per constant energy difference would be nearly flat in the central region, would have a low voltage maximum displaced toward zero, and would have a much lower peak of primary electrons. The shape of the Auger peak would be affected very little.

TABLE I. Summary of measurements of characteristic features.

Material	Test	$V_p^a$ (volts)	$V_1^b$	$V_2^b$ (volts)	$V_3$	$i(\max V_a)^c$ (amp $\times 10^{-14}$ )	$i_b^d$	$R^e$ (percent)	Transition type
Carbon	35	488	276	...	...	1	40	2.5	$V \rightarrow K$
Carbon	36	650	277	...	...	2	36	5.6	$V \rightarrow K$
Carbon	37	771	277	...	...	8	92	8.7	$V \rightarrow K$
Carbon	38	924	277	...	...	14	77	18.2	$V \rightarrow K$
Carbon	39	1210	277	...	...	18	76	23.7	$V \rightarrow K$
Oxygen (NiO)	26	1212	520	...	...	4	85	5	$V \rightarrow K$
Beryllium	59	333	107	...	...	4	16	25	$V \rightarrow K$
Beryllium	61	484	108	...	...	8	24	33	$V \rightarrow K$
Beryllium	62	650	108	...	...	14	34	44	$V \rightarrow K$
Beryllium	63	774	108	...	...	18	34	53	$V \rightarrow K$
Beryllium	64	1070	108	...	...	16	26	62	$V \rightarrow K$
Beryllium oxide	69	775	102	...	...	4	28	14	$V \rightarrow K$
Aluminum	74	640	70	...	...	10	65	16	$V \rightarrow L$
Nickel	13	1075	160	69	...	10	70	14	$V \rightarrow M$
Copper	96	1075	185	63	...	8	57	14	$V \rightarrow M$
Barium	108	1210	94	75	56	20	66	30	$V \rightarrow O$
Platinum	116	1200	91	64	...	8	40	20	$V \rightarrow O$

<sup>a</sup>  $V_p$  = primary beam voltage.

<sup>b</sup>  $V_1, V_2$ , etc. = high voltage edges of features 1, 2, etc.

<sup>c</sup>  $i(\max V_a)$  = maximum current of strongest feature.  $V_1$  in the case of C, O, Be, BaO, Al, Ni;  $V_2$  for Cu, Pt;  $V_3$  for Ba.

<sup>d</sup>  $i_b$  = Average background current for characteristic feature at  $V_a$ .

<sup>e</sup>  $R = 100[i(\max V_a) - i_b]/i_b$ .

<sup>5</sup> W. T. Hughes and J. J. Lander, Rev. Sci. Instr. **24**, 331 (1953).

<sup>6</sup> H. W. B. Skinner, Repts. Progr. Phys. **5**, 257 (1938).

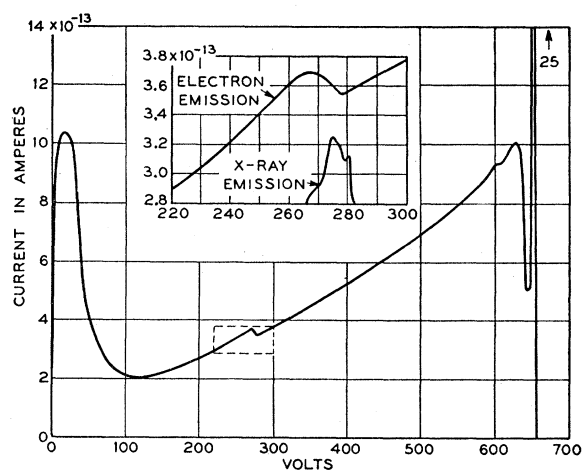


FIG. 3. Secondary electron velocity distribution (not normalized) from carbon. Insert shows Auger peak obtained by amplification, and the soft x-ray emission peak.

The difference in energy between the high voltage edge at 277 volts and that at 282 volts in the curve given by Skinner is largely the result of the effect of the work function of carbon (about 4.5 volts). This energy is lost by the Auger electron in escaping from the surface. The energy difference between the high voltage edge and the maximum is about 11 volts. The corresponding value for the x-ray emission curve is about 7 volts. The long tail on the low voltage side (asymptotic approach to the background) is partly the result of secondary inelastic collisions by primary Auger electrons within the material, as well as the energy range doubling effect described in the introduction. It is probably the most serious experimental limitation to use of the method for obtaining very accurate distributions in energy.

The dependence of the intensity of the feature on primary beam voltage is given in Table I. The ratio  $R$  of the current at the peak maximum ( $i_{\max} - i_b$ ) to the background current  $i_b$  is nearly proportional to  $(V_p - 277)^2$  for low  $V_p$ . Absorption corrections would yield a more complicated form for this dependence.

### 3.2 Oxygen

Oxygen was studied in the form of oxides of several of the metals investigated (Ni, Al, Be, and Ba). The voltage at maximum peak height was about 515, and in all cases the feature was relatively weak (the maximum observed ratio of peak to background was about 0.06, obtained with a primary beam of about 1400 volts). The  $K$  x-ray absorption edge for oxygen is 526 volts, which is interpreted as good agreement with the value 515 for maximum peak height. The shape of the feature was not resolved well enough to justify reproduction. This was due in part to the low intensity of the feature and in part to the lower resolving power of the analyzer in the higher voltage range.

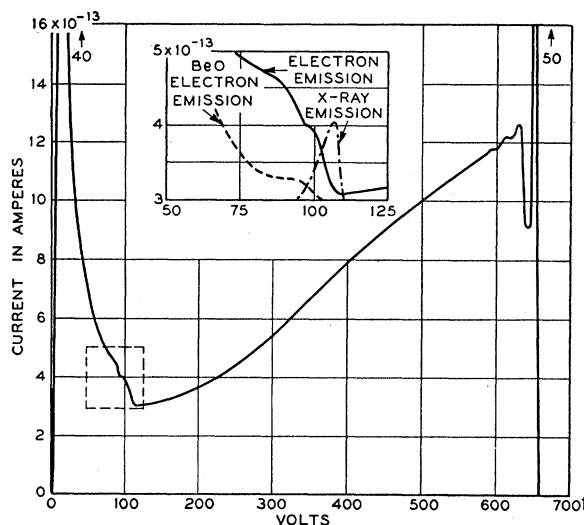


FIG. 4. Secondary electron velocity distribution (not normalized) from beryllium. Insert shows Auger peak obtained by amplification, the soft x-ray emission peak, and the Auger peak obtained from beryllium oxide. The set of peaks near the primary beam (at 660 volts) is the "plasma" feature.

### 3.3 Beryllium

Beryllium produced the strongest of the features observed from different materials. A representative curve is reproduced in Fig. 4. Because of the more complicated nature of this curve, the film of evaporated material (about 100 000 Å thick) was removed after the experiments and analyzed spectrochemically. The analysts reported that it was 99+ percent pure. Patterns obtained from a second evaporation of beryllium agreed well with that given in Fig. 4. Although the beryllium feature is relatively strong, resolution is somewhat limited by the steeply ascending background due to the low voltage secondaries. Note that again the center section of the curve would be nearly flat if plotted on a constant energy difference basis.

A comparison between the distribution of Auger characteristic electrons (due to  $s$  and  $p$  electron transitions) and the x-ray  $K$  band emission data (due largely to  $p$  electron transitions) is also given in Fig. 4. The high voltage edges are in good agreement (108 volts plus the work function, compared with 110 volts). The secondary electron distribution shows a second peak (overlapping band?) with a high voltage edge near 98 volts. The measured variation with primary voltage of the ratio of maximum current of the feature to the average background current is given in Table I.

The double peak in the distribution function is not readily explained as due to overlapping of the  $s$  and  $p$  bands. The distribution calculated by Herring and Hill<sup>7</sup> has too few electrons in the upper section to give the curve observed unless these electrons are highly favored by the transition probabilities. Other possi-

<sup>7</sup> C. Herring and A. G. Hill, Phys. Rev. **58**, 132 (1940).

bilities may be considered, such as amorphous surface structure or surface alloying with an impurity. Further experimental work is desirable.

Oxidation of beryllium yielded a smooth, much less intense, feature with high voltage edge at 102 volts (see Fig. 4).

In the region near the elastically scattered primary beam, peaks were observed which correspond to those reported by Ruthemann.<sup>8</sup> In a distribution curve for secondary electrons obtained by transmission of a beam of electrons of about 7000 volts through beryllium foil, he observed four maxima corresponding to discrete energy losses of 18 volts. We found that slight oxidation changed the character of this region of the curve considerably. The first maximum moved nearer the elastically scattered primary electron peak and the others tended to disappear.

### 3.4 Aluminum

Pure aluminum evaporated on a nickel target yielded a fairly strong feature with edge on the high voltage side at about 70 volts and maximum at about 64 volts. No structure appeared. Resolution of the aluminum peak was poorer than that of beryllium because of the steeply ascending background of low voltage secondaries. The peak is the result of a valence band to *L* transition. The x-ray emission band corresponding to *s* and *d* electron densities and reported by Skinner shows two maxima separated by about 7 volts.

As in the case of beryllium, oxidation was observed to reduce the relative intensity of the feature and displace the maximum toward the low voltage region.

### 3.5 Nickel

A number of features were observed. Two were observed which correspond to transitions of the type  $V \rightarrow M$ . They were moderately intense, one with high voltage edge at 160 volts and maximum at about 152 volts, the second with high voltage edge at 69 and maximum at about 62. A high voltage primary beam (1420 volts) produced two weak features, one with edge at about 816 volts and the other at about 774. They are apparently  $V \rightarrow L$  or  $M \rightarrow L$  type transitions.

### 3.6 Copper

Results similar to nickel were obtained in the  $V \rightarrow M$  type transition range. The features had high voltage edges at 185 volts and 63 volts. Features in the expected range of  $V \rightarrow L$  transitions were not observed.

### 3.7 Barium

The features observed were apparently of type  $V \rightarrow O$ , with edges at 94, 75, and 56 volts.

<sup>8</sup> G. Ruthemann, Ann. Physik 2, 113 (1948).

### 3.8 Platinum

Platinum produced one moderately strong feature with edge at 74 and one weak feature with edge at 91. These are apparently  $V \rightarrow O$  type transitions.

## 4. DISCUSSION

### 4.1 Band Structure Study

The characteristic Auger features observed in the curves for the velocity distributions of secondary electrons have structure analogous in general to that observed in soft x-ray spectra, but differing in detail. A fairly exact theoretical treatment of Auger-type transition probabilities is required in order to interpret this structure in a satisfactory manner. Conversely, the method offers a means of checking a general theory of Auger-type transition probabilities. In addition to the structure of the peaks reported above, it is to be noted that light elements gave the strongest peaks, and this is the theoretically expected result.

The disadvantages more or less inherent to the method are

(a) The complicated nature of the relation between Auger electron distribution and distribution of electrons in the valence band.

(b) A long low voltage tail which is produced by Auger electron secondary energy losses within the material. Some reduction in this tail might be realized by directing the primary beam to the target at a grazing angle of incidence.

(c) Features of interest often occur on a steep background slope produced by low voltage secondaries. Automatic compensation for this slope does not offer a completely satisfactory means of circumventing the difficulty because the exact form of this slope is not readily determinable.

(d) The distribution in velocity of the electrons in the primary beam sets a resolution limit amounting to several tenths of a volt. Beam sources other than tungsten are feasible but much less practical.

Compared with the soft x-ray emission technique, the method has some experimental advantages. Analyses can be made very rapidly, in fact, a feature can conceivably be scanned and displayed on an oscilloscope in a small fraction of a second. The experimental tube is comparatively simple and it can be maintained at extremely low pressures without unusual difficulty. Precision gratings are not needed; measurement is reduced to reading a voltmeter.

### 4.2 Surface Study

It would appear that when primary beams of moderate velocity are used, the yield of characteristic Auger electrons is high for peaks in the low voltage range and for the lighter elements. Most elements can be relied on to yield one or more useful features in this range.

We are essentially interested in those low velocity electrons which have escaped from the target with little energy loss (aside from that due to the external work function). The absorption coefficients for these electrons are very high, and it is clear that electrons will be observed, on the average, from an outer surface layer of the order of ten atoms thick—thicker for atoms of very low atomic number, thinner for atoms of high atomic number.

The data required for an accurate calculation of the sensitivity of the method to surface contamination are not available (see the review of McKay<sup>1</sup>). It is, therefore, of some interest to turn the problem around. The method may be used as a means for determining absorption coefficients with fair accuracy. Consider a surface which yields characteristic electrons in the velocity range desired. Evaporate on this surface at known rate a material whose absorption coefficient is to be studied and bombard continuously with a primary beam of relatively high energy and constant current. Since absorption of the primary beam will be low relative to absorption of the characteristic secondaries, the decay of the intensity of these secondaries with known thickness of evaporated material should provide a reliable measure of the absorption coefficient desired.

In many problems of applied physics and chemistry, the identification of surface composition is at present impossible but of considerable importance. Where the material of interest is present to a depth of several atomic layers and the high vacuum condition is not prohibitive, the method offers a positive means of analysis. Problems of this type can be of widely varied type.

#### 4.3 Distribution in the Region Near the Primary Beam Voltage

The nature and interpretation of the velocity distribution in the region just below the primary beam

has been the subject of considerable study (see McKay,<sup>1</sup> Ruthemann,<sup>8</sup> Rudberg,<sup>9</sup> and Rudberg and Slater<sup>10</sup>). Effects similar to those reported by Ruthemann and interpreted as plasma waves by Pines and Bohm,<sup>11</sup> have been mentioned in Sec. 3.3. Qualitatively similar results were obtained, but the mechanism of discrete energy loss responsible for Ruthemann's results appeared to be much less efficient under the condition of our work (lower beam voltage and reflection rather than transmission). It is, however, of some interest to note that the phenomenon can be observed in the spectrum of reflected electrons. Beryllium gave the strongest features, but comparison of curves obtained with primary beams of 1400 volts and 300 volts showed no significant difference. Aluminum (which, Ruthemann found, gave an excellent series of peaks) yielded two weak peaks. It was observed that superficial oxidation (a monolayer or two) was sufficient to change the character of this region of the curve drastically. Ruthemann also observed peaks at a voltage  $V_p - V_f$ , where  $V_f$  is the voltage of an x-ray type transition (thus  $V_p - 278$  for carbon, and  $V_p - 525$  for oxygen). Such peaks were not seen in the present work.

Results qualitatively comparable to those obtained by Rudberg<sup>9</sup> for Cu, Ba, and BaO were observed. It is to be emphasized that this region is extremely sensitive to surface impurities and that the interpretation of the wide range of velocity distributions which can be obtained appears unusually difficult.

#### ACKNOWLEDGMENT

This work has greatly benefited by discussions between the author and C. Herring, G. Wannier, K. G. McKay, H. Hagstrum, and K. H. Storcks.

<sup>9</sup> E. Rudberg, Phys. Rev. **50**, 48 (1936).

<sup>10</sup> E. Rudberg and J. C. Slater, Phys. Rev. **50**, 150 (1936).

<sup>11</sup> D. Pines and D. Bohm, Phys. Rev. **83**, 221 (1951); **85**, 338 (1952).